CORRECTING FOR TOPOGRAPHY AND FOLIAGE DENSITY IN AN AUTOMATED RADIO TELEMETRY SYSTEM

Kade Jackson

Mentor: Dr. Kristina Fialko, Princeton University
RMBL Education Program, full-time independent research, 2026

ABSTRACT

This project aims to understand the limitations of Automated Radio Telemetry Systems (ARTS) in the context of complex, mountainous landscapes. Environmental variables, such as steep topography, vegetation density, and subject-specific behavior, degrade radio signal strength and localization accuracy. Standard signal decay models frequently fail to account for signal attenuation caused by physical obstructions and complex environmental structures, despite advancements in telemetry technology for wildlife tracking and fine-scale study. Utilizing the existing ARTS grid at the Rocky Mountain Biological Laboratory (RMBL) as a case study, this study aims to identify methods for controlling and accounting for these elevation variations and foliage densities, especially when considering flying organisms such as the Broad-tailed Hummingbird (*Selasphorus platycercus*). Both traditional trilateration and a novel Bayesian particle filter model (equipped with a Generalized Additive Model) were used to estimate point locations given signal strength, time, and node reception, and while trilateration slightly outperformed the new Bayesian model, there remains much to explore in the realm of radio telemetry model development.

INTRODUCTION

Since the 1950s, methods for radio telemetry in biological research have continued to evolve, from primitive transmitters to Automated Radio Telemetry Systems (ARTS) and drone-based tracking (Hockersmith & Beeman, 2012; Manville et al., 2024; Wallace et al., 2021). Radio telemetry technology has revolutionized wildlife conservation by allowing scientists to remotely track free-ranging organisms. By capturing and outfitting animals with transmitters, it has become possible to understand movement at scales previously unfathomable, including the mapping of international migration routes, the identification of critical corridors, and gaining a better understanding of how organisms navigate human-altered landscapes (Bastille-Rousseau et al., 2018; Dzul et al., 2024; Kishkinev et al., 2016; Mitchell et al., 2025; Oliver et al., 2026). Recent advancements, such as minuscule radio tags intended for butterflies or hummingbirds, have further facilitated this study of movement at even finer scales (Heitzler et al., 2025; Rhodes et al., 2025, Preprint). Despite these technological advancements, relatively little research exists on how each of these different forms of information interact with a radio telemetry grid at both broad and fine scales.

The technical aspects of radio telemetry often consist of radio waves (VHF/UHF) transmitted from attached tags or collars to receivers, enabling continuous data collection over time. These radio waves transmit high-frequency electromagnetic data over long distances by propagating through the environment. Receiving antennas, or grid nodes, capture these waves, converting them back into usable data for monitoring, tracking, or environmental sensing (Amelon et al., 2009; Fuller, 1987; Manville et al., 2024). In ARTS grid systems, data is received as the signal strength per radio tag per node, which is then used to understand an animal’s physical location after accounting for the grid's calibration (Wallace et al., 2021). However, due to the nature of these waves, there exist many confounding factors impacting signal reception, including terrain ruggedness, subject height, and vegetation type/density (Rueda-Uribe et al., 2024).

Land topography and elevation have been shown to result in substantial effects on signal reception, as nodes with greater or obstructed vertical distance from a radio tag often receive weaker signals, resulting in a greater calculated distance than the actual value (Rueda-Uribe et al., 2024; Tran et al., 2024). When a signal loses line of sight, the received signal strength (RSS) drops abruptly, mimicking an increase in horizontal distance even if the subject is located near the receiver (Tran et al., 2024; Whitehouse et al., 2007). If the localization algorithm assumes a flat two-dimensional plane, this attenuation can overstate the horizontal distance between the node and the subject, impacting the ability to accurately determine the subject's location (Tran et al., 2024). As most calibrated grids have a detection threshold or signal sensitivity limit, extreme vertical distance or terrain obstruction may result in negative skew of signal strength, which may be filtered out after accounting for a typical decay curve (Tran et al., 2024; Wallace et al., 2021; Whitehouse et al., 2007). Steep topographic features can completely obstruct the line of sight, preventing nodes from detecting a signal entirely even if the horizontal distance is minimal (Rueda-Uribe et al., 2024; Tran et al., 2024). This logic also extends to aerial organisms, as the subject's vertical distance from a node and elevation have very similar impacts on signal strength (Rueda-Uribe et al., 2024). While altitude provides a better practical line of sight, the vertical distance a signal must cover from high altitudes will dilute the signal strength (Khawaja et al., 2019). If an organism is flying high enough, the attenuated signal will eventually fall below the grid's calibration threshold.

Vegetation type and density can also impact signal strength, weakening reception in denser areas or areas occupied by certain foliage types (Gamble et al., 2025; Tran et al., 2024). In structurally complex environments, vegetation reduces accuracy through shadowing and multipath reflection (where signals bounce off foliage or ground cover), causing the receiver to misinterpret the signal's origin and strength (Paxton et al., 2022). In a study on songbird locations in a forested environment, RSS obstruction increased alongside tree density (Gamble et al., 2025). Telemetry localization relies on probability models where signal degradation is proportional to the square of the distance from the subject to the receiver, yet standard continuous signal decay models often fail in complex habitats (Erhardt et al., 2023; Wallace et al., 2022). Signal decay function parameters have been found to significantly differ by habitat type, requiring habitat- or density-specific adjustments, such as localized calibration grids, Bayesian signal decay models, or stringent signal-to-noise filtering, to improve location accuracy (Paxton et al., 2022; Rueda-Uribe et al., 2024; Tran et al., 2024).

Beyond environmental structure, the behavioral ecology of the study system or species may dictate the accuracy of radio signal reception. As an example, male Broad-tailed Hummingbirds (*Selasphorus platycercus*) are characterized by high-speed, vertical aerial display dives; this drastic variation in vertical space causes signals to travel along differing slant ranges and frequently results in the bird traversing past threshold zones of receiving antennas (Camfield et al., 2020; Clark et al., 2011; Khawaja et al., 2019; Rueda-Uribe et al., 2024). Alternatively, female hummingbirds spend significantly more time skulking, foraging, and nesting deep within tree canopies or dense shrubs (Camfield et al., 2020). This behavior subjects their radio tags to severe shadowing and multipath reflection from the surrounding biomass, which may further degrade RSS (Paxton et al., 2022; Gamble et al., 2025). Tracking small mammals also presents a unique challenge because of their ground-dwelling nature: proximity to the ground results in radio waves that are heavily absorbed and scattered by soil moisture, rocks, and underbrush, potentially reducing both the effective transmission range and the reliability of the RSS data (Wallace et al., 2022).

Despite these findings, there exists little research examining the impact of more severe topographic differences in mountainous environments. At the Rocky Mountains Biological Laboratory (RMBL) in Gothic, Colorado, an ARTS system is utilized to track male Broad-tailed Hummingbirds (*Selasphorus platycercus*) during their breeding season from spring to late summer. While there are many implications for this research, the grid currently exists as a series of ~100m linearly separated nodes. This linear separation is likely obscuring collected data, especially given that there is elevational variation in node placement and differing foliage types and densities across the study sites, yet RSS is implicitly a linear factor. To further enhance and clarify this research, this project serves to both understand how the relationship between signal strength and distance from node is impacted by these factors, as well as to present an alternative data processing methodology that takes into account both land topography and foliage density. These findings may be useful across other study systems as well and will inform future researchers of how best to approach analyzing RSS values in heterogeneous landscapes.

METHODOLOGY

Existing RSS-based automated telemetry studies often estimate tag/subject locations using trilateration or radio fingerprinting (Paxton et al., 2022; Tyson et al., 2024). However, these approaches do not incorporate probabilistic movement models or Bayesian sequential estimation, despite the success of particle filters in RSS localization (Doucet et al., 2001; Thrun et al., 2005). Additionally, particle filters have been shown to outperform trilateration when RSS measurements are noisy and/or sensor geometry is poor, although these demonstrations largely come from engineering rather than wildlife studies (Lee et al., 2025).

To obtain an accurate picture of the landscape, I established a linear 20m x 20m grid encompassing each node/receiver location with a 100m buffer zone, akin to the fingerprinting proposed by Tyson et al. (2024) (Figure 1). I visited each point with a test tag for two minutes at two vertical strata: one minute at 0m and the other at 2.55m, to account for hummingbird flight heights. To account for on-foot travel time between differing points, as well as to give the tag time to adjust to the new location, the first and last fifteen seconds of each minute were removed from the calibration dataset. Each point’s location was recorded, along with the RSS from each node (and that node’s location). Landscape data were integrated using LiDAR from the general area, including a Digital Elevation Model (DEM) and a foliage cover/density model. Each grid point was then characterized by its distance from the receiving node as well as the foliage density at that geographic location. Additional metrics (line-of-sight and terrain obstruction between each calibration point and receiver) were also extracted from the DEM as needed to account for signal attenuation impacted by the local topography (Jenness, 2004).

To characterize radio signal propagation and establish the spatial limits of the automated radio telemetry system, I analyzed calibration data collected from known reference positions. I calculated Euclidean distances between each calibration point and its corresponding receiving node. To model signal attenuation, I fitted a standard log-distance path loss model to the empirical data using linear regression of Received Signal Strength (RSS) against log(d). From this regression, I derived the baseline signal strength at 1 meter and the environmental path loss exponent. To determine the limits of distance estimation (where signal propagation breaks down), I implemented segmented regression/breakpoint analysis using the segmented package in R. This was used to fit a multi-segment linear model to the log-distance decay curve to mathematically identify the inflection point, or breakpoint distance. I then computed the RSS value corresponding to this breakpoint to establish a cutoff for filtering unreliable low-signal detections prior to spatial modeling.

I then utilized a Generalized Additive Model (GAM) to predict expected signal strength based on the log-distance to the receiving node, topography, and foliage density. Rather than predicting a single RSS value, the GAM estimated the expected distribution of RSS, including residual variance, to allow for measurement uncertainty to be incorporated into the localization (Wood, 2017; Heim et al., 2018). Received data (after filtering for background noise/unusable detections) were smoothed to reduce temporal signal jitter using a Kalman filter applied within a state-space model, which recursively estimates the underlying signal while accounting for measurement noise (Welch & Bishop, 2006).

After running the GAM to obtain the array of expected signal strengths at each grid point, I applied a geographically bounded Bayesian particle filter with the ability to process simultaneous pulse detections to determine each detected tag's 3D coordinates (Doucet et al., 2001; Thrun et al., 2005). In short, the tag's location is represented by a probability cloud of simulated particles. For each particle, the likelihood was calculated using the probability of observing the measured RSS values at all simultaneously detecting receivers, given the GAM-predicted RSS distribution for that particle's 3-D coordinate (x, y, z). Particles were resampled based on likelihood weights, and a correlated random-walk movement model, scaled to the maximum movement speed of the target species, will provide the prior probability of movement between successive detections (Codling et al., 2008; Patterson et al., 2008). The final estimated coordinate is the weighted posterior mean of the particle cloud rather than a simple arithmetic mean (Doucet et al., 2001; Thrun et al., 2005).

The coordinates provided by both the bounded L-BFGS-B trilateration and the new Bayesian model were then compared to the actual values through further grid testing (random points) to determine the most accurate model for the RMBL area. I utilized a non-parametric Wilcoxon signed-rank test along with a parametric paired t-test to analyze each model's location accuracy when compared to the actual latitude/longitude values. Furthermore, I tested the height accuracy of the Bayesian particle filter with a one-sample t-test to determine if the vertical discrepancy was significantly different from zero.

RESULTS

After obtaining the distance decay model and running the segmented regression analysis, the calculated breakpoint distance of the calibration model was 92.39 meters, and the calculated RSS cutoff was around -81.57 dBm (Figure 2).

The Generalized Additive Model (GAM) used to train the Bayesian particle filter yielded an R-squared value of 0.56 and a residual error of 3.83. Geographically bounded L-BFGS-B trilateration yielded a mean positional error of 58.85 m (RMSE = 75.26 m), while the Bayesian particle filter produced a mean error of 71.67 m (RMSE = 135.63 m). The larger RMSE for the Bayesian model likely indicates a right-skewed error distribution driven by occasional massive spatial outliers, as visible in Figure 3. Because of these outliers, a Wilcoxon signed-rank test was utilized to compare model performance. This test revealed a statistically significant difference in positional accuracy between the two methodologies ($V = 10045$, $p = 0.006$); L-BFGS-B trilateration provided consistently lower median spatial errors. A paired t-test resulted in a mean difference of 12.82 m, though this was interestingly non-significant ($t(224) = 1.95$, $p = 0.052$, 95% CI [-0.13, 25.76]).

On average, the Bayesian particle filter exhibited a slight negative bias on its vertical height predictions, underestimating true height by a mean of around 1.67 m. The overall mean absolute height error was 4.29 m (RMSE = 6.94 m). A one-sample t-test confirmed that the -1.67 m underestimation was statistically significantly different from zero ($t(234) = -3.79$, $p = 0.0002$, 95% CI [-2.54, -0.80]).

DISCUSSION

While Bayesian particle filters (BPF) generally integrate movement dynamics with spatial data, traditional trilateration proved to maintain superior accuracy with this grid system and model integration. The high RMSE value from the BPF reveals a high volume of spatial outliers, which likely contributed to this result. The lack of significance comparing the models under a parametric two-sided t-test is especially interesting, as it implies that there is at least some level of overlap between the models' efficacies, even though the trilateration severely overperformed. It is entirely possible that, given more time and resources, BPF could surpass trilateration even in this system. BPF training during data analysis proved to heavily skew points toward places with higher line-of-sight and slopes/aspects that allowed for maximum theoretical node overlap, despite not being represented in the calibration points as such. Removing slope and aspect slightly lowered the R-squared fit of the final model, but it is still unclear which other factors should be included, or even how to correct for biases like slope and aspect within the model, rather than just removing their influence. Furthermore, there exist many methods of particle filtering, and it is possible that the method employed was flawed or otherwise not ideal for this particular system. Investing time into properly understanding and executing a location-based Bayesian inference system may indeed prove more useful than relying on trilateration, although trilateration is exceedingly simpler than developing a model. Still, trilateration only provided an accuracy of around 70m, which is also lower than expected given the 20m x 20m setup for calibration. This may have varied with a more traditional trilateration setup, but time and weather constraints prevented this (and the completion of the Bayesian grid itself) from occurring.

Environmental aspects may have also led to these results. Land topography, elevation shifts, and varying vegetation density can cause signal attenuation and multipath/“bounce” effects, in which the signal from the transmitting tag travels differently given the local environment (Frair et al., 2010; Gamble et al., 2025; Paxton et al., 2022; Rueda-Uribee et al., 2024; Tran et al., 2024). While trilateration treats each localization independently (and each tag is localized between at least three nodes), Bayesian models rely on prior locations and movement models. If a severe multipath error occurs, or if vegetation heavily skews signal reception at multiple automated nodes, a BPF can trap particles in the wrong topographical area (Figure 4). While removing slope and aspect prevented the piling of these points on top of the nearest ridge in my own model, large spatial outliers still existed within the model. My model’s high RMSE doesn’t necessarily imply that Bayesian models are inferior to trilateration; rather, it suggests that the model didn’t properly function when taking into account the environmental variables present, either GAM-present or ignored/not recognized.

Furthermore, the choice between different models and algorithms dictates the types of ecological questions that can be answered. If a study relies on identifying precise micro-habitats, trilateration’s resistance to movement-model errors might lend itself to being the most practical application in that context (Patterson et al., 2008). Conversely, if studying broad, continuous behavioral shifts, the BPF's ability to smooth trajectories might still be valuable, provided that researchers pre-filter the raw data to restrict anomalous spatial jumps before applying the Bayesian framework, or utilize the model to account for these potential outliers, since animal movements don’t typically follow a set mathematical formula. Additionally, BPF models have been shown to be incredibly accurate when used as movement modeling rather than just accepting point values; perhaps there is some utility in exploring the utilization of BFPs in conjunction with trilateration rather than treating BPFs as an equivalent (Lavender et al., 2025).

With that being said, I propose future projects implement a hybrid approach when working with large-scale ARTS systems like the one present at RMBL. This could be achieved very simply, where trilateration is used to identify multipath outliers that can be removed before the BFP is applied, or it could be used in a more integrated way, in which both trilateration measurements and BFP predictions are combined in a separate, larger-scale model. It is also possible that my own approach is valid, and I didn’t have enough data to properly integrate terrain, foliage cover, and node data. The initial calibration grid was planned to include around 1,000 points; around 350 were collected, and due to weather conditions only around 250 calibration points were recorded in the final product. Perhaps a larger grid would provide the resolution needed to adequately integrate a GAM with these environmental factors. This would minimize potential blind spots in the BFP and would allow for a greater array of terrain/vegetation combinations, which my grid may not have included at the scale necessary to properly understand these varying impacts.

LITERATURE CITED

Amelon, S. K., Dalton, D. C., Millspaugh, J. J., & Wolf, S. A. (2009). Radiotelemetry; techniques and analysis. *In: Kunz, Thomas H.; Parsons, Stuart, Eds. Ecological and Behavioral Methods for the Study of Bats. Baltimore: Johns Hopkins University Press: 57-77.*, 57–77.

Bastille-Rousseau, G., Wall, J., Douglas-Hamilton, I., & Wittemyer, G. (2018). Optimizing the positioning of wildlife crossing structures using GPS telemetry. *Journal of Applied Ecology*, *55*(4), 2055–2063. https://doi.org/10.1111/1365-2664.13117

Bishop, G. (n.d.). *An Introduction to the Kalman Filter*.

Camfield, A. F., Calder, W. A., & Calder, L. L. (2020). Broad-tailed Hummingbird (Selasphorus platycercus), version 1.0. *Birds of the World*. https://doi.org/10.2173/bow.brthum.01

Clark, C. J., Elias, D. O., & Prum, R. O. (2011). Aeroelastic Flutter Produces Hummingbird Feather Songs. *Science*, *333*(6048), 1430–1433. https://doi.org/10.1126/science.1205222

Codling, E. A., Plank, M. J., & Benhamou, S. (2008). Random walk models in biology. *Journal of The Royal Society Interface*, *5*(25), 813–834. https://doi.org/10.1098/rsif.2008.0014

Doucet, A., Freitas, N., & Gordon, N. (Eds.). (2001). *Sequential Monte Carlo Methods in Practice*. Springer. https://doi.org/10.1007/978-1-4757-3437-9

Dzul, M. C., Kendall, W. L., Yackulic, C. B., Van Haverbeke, D. R., Mackinnon, P., Young, K., Pillow, M. J., & Thomas, J. (2024). Estimating migration timing and abundance in partial migratory systems by integrating continuous antenna detections with physical captures. *Journal of Animal Ecology*, *93*(7), 796–811. https://doi.org/10.1111/1365-2656.14076

Erhardt, S., Koch, M., Kiefer, A., Veith, M., Weigel, R., & Koelpin, A. (2023). Mobile-BAT—A Novel Ultra-Low Power Wildlife Tracking System. *Sensors*, *23*(11), 5236. https://doi.org/10.3390/s23115236

Frair, J. L., Fieberg, J., Hebblewhite, M., Cagnacci, F., DeCesare, N. J., & Pedrotti, L. (2010). Resolving issues of imprecise and habitat-biased locations in ecological analyses using GPS telemetry data. *Philosophical Transactions of the Royal Society B: Biological Sciences*, *365*(1550), 2187–2200. https://doi.org/10.1098/rstb.2010.0084

Fuller, M. R. (1987). *Applications and Considerations for Wildlife Telemetry*.

Gamble, M. D., Raginski, N. M., & Long, A. M. (2025). Field methods to improve received signal strength (RSS)–based localization for tracking songbird movements in forests. *Journal of Field Ornithology*, *96*(4). https://doi.org/10.5751/JFO-00680-960406

Heim, K. C., Steeves, M. E., McMahon, T. E., Ertel, B. D., & Koel, T. M. (2018). Quantifying Uncertainty in Aquatic Telemetry: Using Received Signal Strength to Estimate Telemetry Error. *North American Journal of Fisheries Management*, *38*(5), 979–990. https://doi.org/10.1002/nafm.10226

Heitzler, S., Dallmöller, S., Hinneberg, H., Murillo-Hiller, L. R., & Gottschalk, T. K. (2025). Radio telemetry of butterflies: Practical insights and critical tag-weight thresholds. *Movement Ecology*, *13*, 86. https://doi.org/10.1186/s40462-025-00615-9

Hockersmith, E., & Beeman, J. (2012). *A History of Telemetry in Fishery Research* (pp. 7–19).

Jenness, J. S. (2004). Calculating landscape surface area from digital elevation models. *Wildlife Society Bulletin*, *32*(3), 829–839. https://doi.org/10.2193/0091-7648(2004)032%255B0829:CLSAFD%255D2.0.CO;2

Khawaja, W., Guvenc, I., Matolak, D. W., Fiebig, U.-C., & Schneckenburger, N. (2019). A Survey of Air-to-Ground Propagation Channel Modeling for Unmanned Aerial Vehicles. *IEEE Communications Surveys & Tutorials*, *21*(3), 2361–2391. https://doi.org/10.1109/COMST.2019.2915069

Kishkinev, D., Heyers, D., Woodworth, B. K., Mitchell, G. W., Hobson, K. A., & Norris, D. R. (2016). Experienced migratory songbirds do not display goal-ward orientation after release following a cross-continental displacement: An automated telemetry study. *Scientific Reports*, *6*(1), 37326. https://doi.org/10.1038/srep37326

Lavender, E., Scheidegger, A., Albert, C., Biber, S. W., Illian, J., Thorburn, J., Smout, S., & Moor, H. (2025). Particle algorithms for animal movement modelling in receiver arrays. *Methods in Ecology and Evolution*, *16*(8), 1808–1819. https://doi.org/10.1111/2041-210X.70028

Lee, H., Park, J., & Park, K. (2025, August 19). *Evaluating Particle Filtering for RSS-Based Target Localization under Varying Noise Levels and Sensor Geometries*. arXiv.Org. https://arxiv.org/abs/2508.13937v2

Manville, A. M., Levitt, B. B., & Lai, H. C. (2024). Health and environmental effects to wildlife from radio telemetry and tracking devices—State of the science and best management practices. *Frontiers in Veterinary Science*, *11*, 1283709. https://doi.org/10.3389/fvets.2024.1283709

Mitchell, L., Brust, V., Karwinkel, T., Åkesson, S., Kishkinev, D., Norevik, G., Szep, T., Hedenström, A., Lagerveld, S., Helm, B., & Schmaljohann, H. (2025). Conservation-focused mapping of avian migratory routes using a pan-European automated telemetry network. *Conservation Biology*, *39*(4), e70017. https://doi.org/10.1111/cobi.70017

Oliver, R., Yanco, S., Ellis Soto, D., Jesmer, B., Cohen, J., Gao, S., Patchett, R., Avgar, T., Bildstein, K., Bakner, N., Barber, D., Barker, K., Barnes, J., Bastille-Rousseau, G., Belant, J., Benson, J., Bêty, J., Beyer, D., David, & Jetz, W. (2026). Interacting effects of human presence and landscape modification on birds and mammals. *Science*, *392*, 879–884. https://doi.org/10.1126/science.adq3396

Patterson, T. A., Thomas, L., Wilcox, C., Ovaskainen, O., & Matthiopoulos, J. (2008). State-space models of individual animal movement. *Trends in Ecology & Evolution*, *23*(2), 87–94. https://doi.org/10.1016/j.tree.2007.10.009

Paxton, K. L., Baker, K. M., Crytser, Z. B., Guinto, R. M. P., Brinck, K. W., Rogers, H. S., & Paxton, E. H. (2022). Optimizing trilateration estimates for tracking fine-scale movement of wildlife using automated radio telemetry networks. *Ecology and Evolution*, *12*(2), e8561. https://doi.org/10.1002/ece3.8561

Rhodes, E. M., Burcher, S., Johnson, E., Contreras-Martínez, S., Puma, D. A. L., Shepard, K., Williams, D., & Lanzone, M. (2025). *Ultralight Solar Transmitter Enables Fine-Scale Movement Ecology in North American Hummingbird Migration* (p. 2025.12.29.696924). bioRxiv. https://doi.org/10.64898/2025.12.29.696924

Rueda-Uribe, C., Sargent, A. J., Echeverry-Galvis, M. Á., Camargo-Martínez, P. A., Capellini, I., Lancaster, L. T., Rico-Guevara, A., & Travis, J. M. J. (2024). Tracking Small Animals in Complex Landscapes: A Comparison of Localisation Workflows for

Automated Radio Telemetry Systems. *Ecology and Evolution*, *14*(10), e70405. https://doi.org/10.1002/ece3.70405

Thrun, S., Burgard, W., & Fox, D. (2005). *Probabilistic Robotics*. MIT Press.

Tran, V., Vitz, A., & Bakermans, M. (2024). Evaluating habitat-specific interference in automated radio telemetry systems: Implications for animal movement studies. *Animal Biotelemetry*, *12*. https://doi.org/10.1186/s40317-024-00369-y

Tyson, C., Fragueira, R., Sansano-Sansano, E., Yu, H., & Naguib, M. (2024). Fingerprint localisation for fine-scale wildlife tracking using automated radio telemetry. *Methods in Ecology and Evolution*, *15*(11), 2118–2128. https://doi.org/10.1111/2041-210X.14410

Wallace, G., Elden, M., Boucher, R., & Phelps, S. (2022). An automated radiotelemetry system (ARTS) for monitoring small mammals. *Methods in Ecology and Evolution*, *13*(5), 976–986. https://doi.org/10.1111/2041-210X.13794

Whitehouse, K., Karlof, C., & Culler, D. (2007). A practical evaluation of radio signal strength for ranging-based localization. *Mobile Computing and Communications Review*, *11*, 41–52. https://doi.org/10.1145/1234822.1234829

Wood, S. N. (2017). *Generalized Additive Models: An Introduction with R, Second Edition* (2nd ed.). Chapman and Hall/CRC. https://doi.org/10.1201/9781315370279

APPENDIX

Figure 1: 20m x 20m calibration grid and node locations.

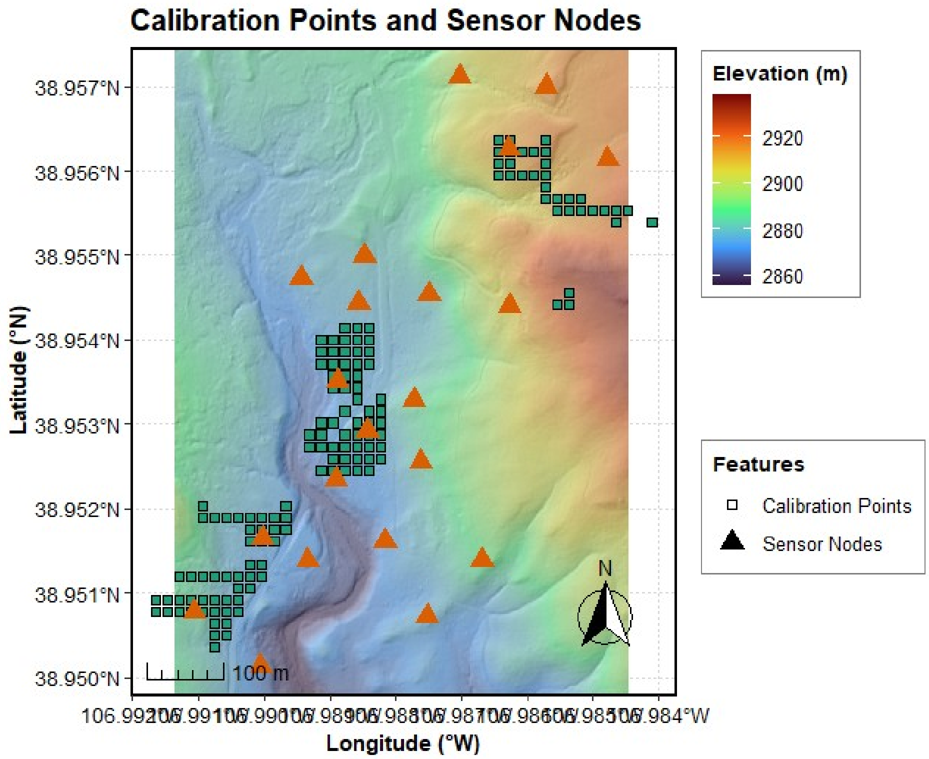

Figure 2: Signal decay curve from calibration grid. Calculated breakpoint distance: 92.39 meters; calculated RSS cutoff: -81.57 dBm.

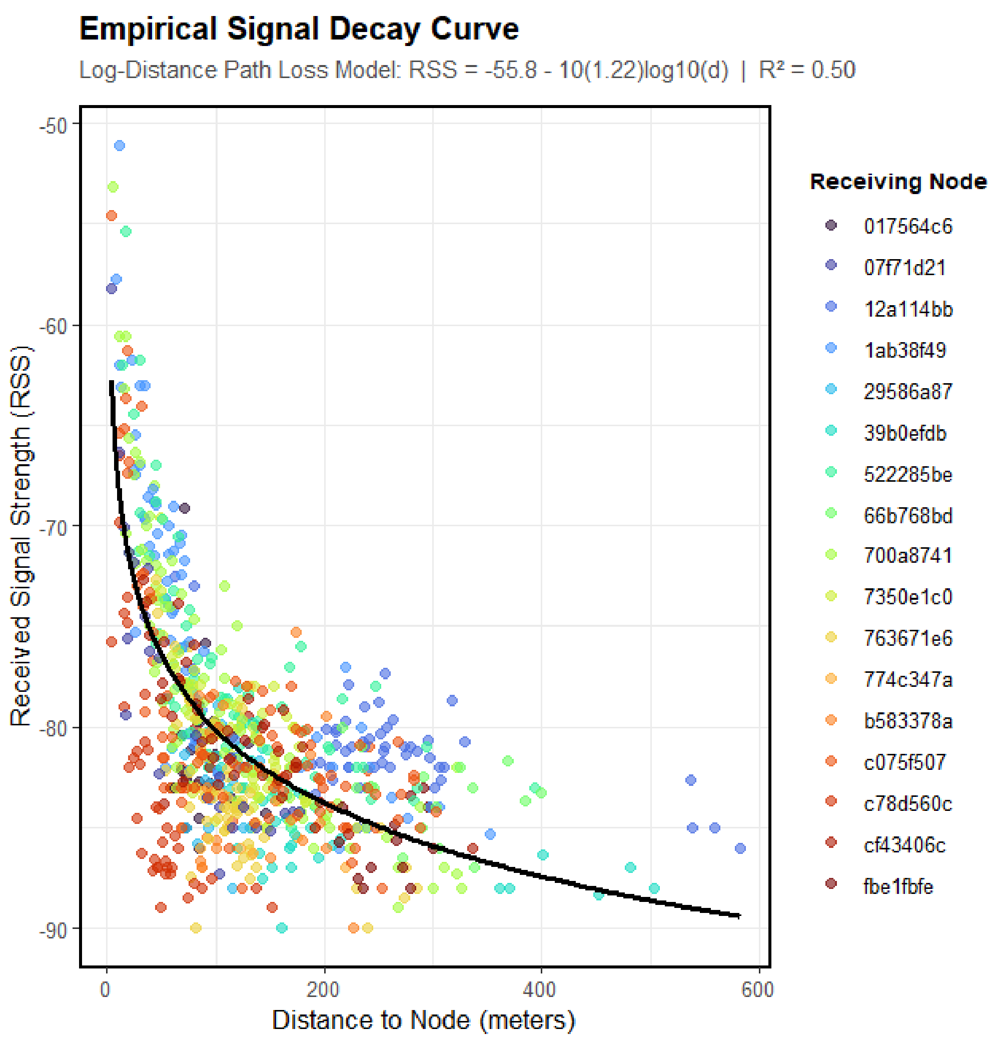

Empirical Signal Decay Curve
Log-Distance Path Loss Model: RSS = -55.8 - 10(1.22)log10(d) | R² = 0.50
Received Signal Strength (RSS)
-50
-60
-70
-80
-90
0
200
400
600
Distance to Node (meters)
Receiving Node
017564c6
07f71d21
12a114bb
1ab38f49
29586a87
39b0efdb
522285be
66b768bd
700a8741
7350e1c0
763671e6
774c347a
b583378a
c075f507
c78d560c
cf43406c
fbe1fbfe

Figure 3: Final map of all BFP-predicted, trilateration-predicted, and actual tag points in the RMBL area.

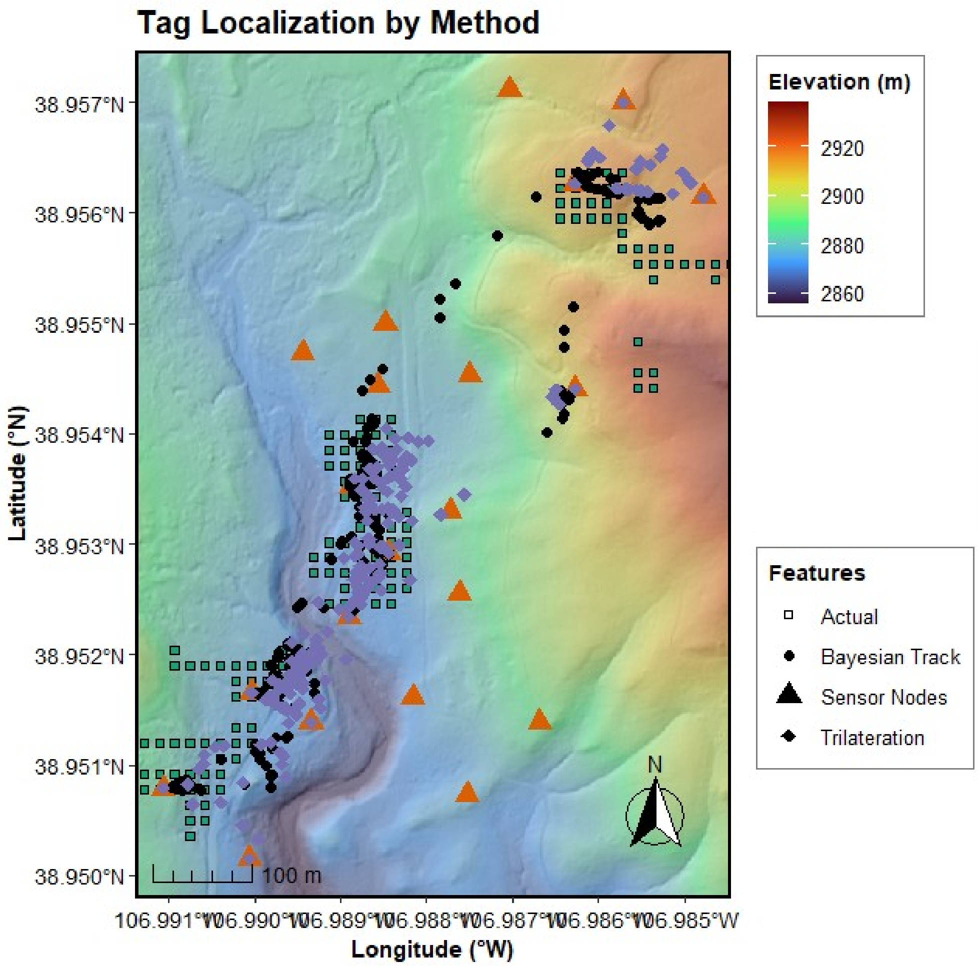

Figure 4: Demonstration map of BFP point piling as a result of a possible large-scale multipath error; this was later corrected by the removal of slope and aspect entirely.